Hyperfine field assessment of the magnetic structure of $ZrZn_2$

A. V. Tsvyashchenko*
Vereshchagin Institute for High Pressure Physics, RAS, 142190 Moscow, Troitsk, Russia
and Skobeltsyn Institute Of Nuclear Physics Lomonosov Moscow State University, Leninskie Gory, Moscow 119991, Russia

D. A. Salamatin
Vereshchagin Institute for High Pressure Physics, RAS, 142190 Moscow, Troitsk, Russia
and Moscow Institute of Physics and Technology, 141700 Dolgoprudny, Russia

A. Velichkov, A. V. Salamatin, and V. N. Trofimov
Joint Institute for Nuclear Research, Dubna, P.O. Box 79, Moscow, Russia

L. N. Fomicheva, V. A. Sidorov, and A. V. Fedorov
Vereshchagin Institute for High Pressure Physics, RAS, 142190 Moscow, Troitsk, Russia

A. V. Nikolaev
Skobeltsyn Institute of Nuclear Physics Lomonosov Moscow State University, Leninskie Gory, Moscow 119991, Russia
and Moscow Institute of Physics and Technology, 141700 Dolgoprudny, Russia

G. K. Ryasny and A. V. Spasskiy
Skobeltsyn Institute of Nuclear Physics Lomonosov Moscow State University, Leninskie Gory, Moscow 119991, Russia

M. Budzynski
Institute of Physics, M. Curie-Sklodowska University, 20-031 Lublin, Poland
(Received 19 June 2014; revised manuscript received 3 February 2015; published 24 March 2015)

Time differential perturbed $\gamma\gamma$ angular correlation spectroscopy on ^{111}Cd nuclei probes inserted in $ZrZn_{1.9}$ is used to measure the magnetic hyperfine fields at Zr and Zn sites and the electric-field gradient V_{zz} at Zn sites as a function of temperature at various pressures and as a function of pressure at the temperature 4 K. Our data indicate that the local magnetic moment of Zr in the magnetically ordered state is substantially larger than its value obtained from the macroscopic measurements. The transformation between paramagnetic and magnetically ordered states is considered as a fluctuation-induced first-order transition. We conclude that $ZrZn_2$ is not a simple ferromagnet and discuss a possible type of its magnetic ordering.

DOI: 10.1103/PhysRevB.91.104423 PACS number(s): 76.80.+y, 75.25.−j, 71.70.Jp

I. INTRODUCTION

Itinerant ferromagnetism attracts substantial interest despite its being relatively less common. This interest is largely triggered by interesting and not yet fully understood phenomena that occur when the order is suppressed at zero temperature by pressure or other means. Such quantum phase transitions (QPTs) are driven by quantum fluctuations rather than thermal ones, and the transition itself represents a quantum critical point (QCP). In the vicinity of the quantum critical point novel and nontrivial phenomena emerge, such as non- Fermi-liquid behavior [1], triplet superconductivity [2–6], skyrmion phases, and the topological Hall effect [7,8].

$ZrZn_2$ is a prototypical itinerant ferromagnet, and it exhibits a first-order QPT at the critical pressure $p_c = 16.5$ kbar, in accord with the metamagnetic behavior, characterized by a sudden superlinear rise in the magnetization as a function of applied field, for pressures above p_c [9].

$ZrZn_2$ crystallizes in the $C15$ cubic Laves structure, the space group is $Fd3m$; see Fig. 1. At ambient pressure the ferromagnetic order sets in at the Curie temperature T_C = 23–28 K. Magnetization measurements indicate a small net magnetic moment of 0.13–0.23μ_B per formula unit, while the intermediate-temperature susceptibility can be fitted by the Curie-Weiss law with the effective moment 1.9μ_B [9,10]. Not unusual for itinerant magnets, the overall temperature dependence is not Curie-Weiss; as the temperature grows above the room temperature, the effective moment is reduced and the Curie-Weiss temperature increases compared to T_C. Unlike UGe_2 [11] and MnSi [12–14], the magnetic structure of $ZrZn_2$ has not been successfully characterized by neutron diffraction. Neutron scattering on high quality samples of $ZrZn_2$ have provided the only direct experimental evidence on the nature of the spin density [15,16] and low-lying magnetic excitations [17]. They have confirmed the itinerant nature of spin polarization, as the latter is delocalized along the network of Zr atoms with the maximum polarization at the middle of Zr-Zr bonds. The existence of a magnetic short-range order in $ZrZn_2$ however has been confirmed by nuclear magnetic resonance (NMR) on the ^{91}Zr nuclei [18–20]. In addition, a local magnetic hyperfine field (MHF) at the Zr site was reported in a few studies [21,22] allowing us to estimate the value of its magnetic moment.

*tsvyash@hppi.troitsk.ru

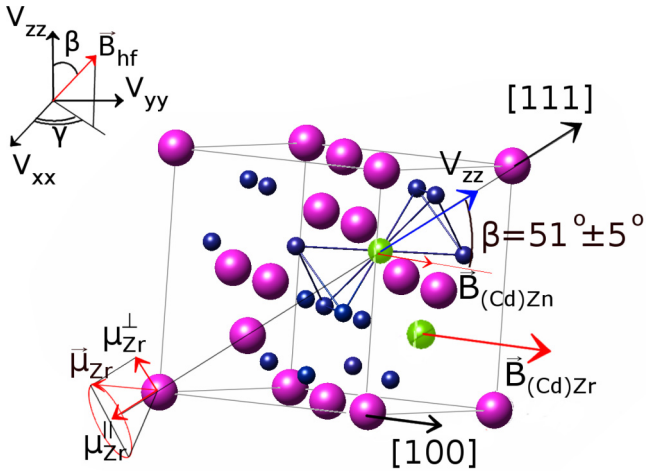

FIG. 1. (Color online) The $C15$ crystal structure of $ZrZn_2$ (the $MgCu_2$ lattice type). Zirconium atoms are represented by large (magenta) spheres, zinc atoms by small (navy) spheres, and ^{111}Cd probes by medium-sized (green) spheres, which can occupy sites of Zr and Zn. Arrows indicate the directions of the magnetic hyperfine fields $B_{(Cd)Zn}$, $B_{(Cd)Zr}$ and the magnetic moment of the zirconium ion ($\mu_{Zr} = 0.5\mu_B$/at. Zr). The magnetic hyperfine fields $B_{(Cd)Zn}$, $B_{(Cd)Zr}$ are measured at ^{111}Cd probes located at zinc and zirconium sites, respectively. The inset shows the angles β and γ giving the direction of the magnetic hyperfine field in the coordinate system defined by the EFG tensor.

While it is generally accepted that $ZrZn_2$ is a uniform ferromagnet with all Zr atoms carrying the same (small) magnetization, existing neutron-scattering experiments [15,16] were primarily aimed at distinguishing between the localized and itinerant magnetism, and cannot exclude with certainty a possibility of a sign change, for instance, a long-pitch spiral.

Remarkably, a magnetic component of the opposite sign, that is, the antiferromagnetic component, has been unambiguously detected in the $ZrZn_2$ powder sample in the zero-field muon spin rotation (μSR) experiments [23]. The μSR data imply that the magnetically ordered phase of $ZrZn_2$ is not a simple ferromagnet.

It is also worth noting that the standard density functional theory (DFT) in the local-density approximation (LDA) results in a large magnetic moment [24] of $0.72\mu_B$ per formula unit (f.u.) for $ZrZn_2$. This value is nearly four times larger than the established experimental moment. In Ref. [24] this fact is accounted for by fast spin fluctuations averaged with the help of Moria's self-consistent renormalization procedure.

In the present work we report the magnetic hyperfine fields at zirconium and zinc sites and the electric-field gradient (EFG) at Zn sites of $ZrZn_{1.9}$ measured by means of time-differential perturbed angular correlations (TDPACs) spectroscopy at the ^{111}Cd probe nucleus which has a close electron shell in the lattice. The ^{111}Cd probe nuclei were inserted in the $ZrZn_{1.9}$ lattice and were detected at both zirconium (Zr) and zinc (Zn) sites of $ZrZn_{1.9}$ crystallized in the $C15$ cubic Laves structure (as $ZrZn_2$; Fig. 1). The experiments have been carried out at low temperatures with applied pressure up to 2 GPa.

Note that the hyperfine spectroscopic techniques such as TDPAC, Mössbauer, NMR, and others are very sensitive to inhomogeneities of the magnetic properties, which is their very important advantage. In particular, TDPAC spectroscopy measuring short-ranged hyperfine interactions (magnetic or electric) results in a nanometer special resolution and can identify different local configurations in the same sample. Unlike macroscopic techniques that measure averaged quantities such as magnetization, resistivity, etc., TDPAC is a microscopic method that can determine local variations of magnetic moment and exchange.

The paper is organized as follows. In Sec. II we give experimental details of the TDPAC measurements, in Sec. III we analyze our data on $ZrZn_{1.9}$, and in Sec. IV we present the summary of our work.

II. EXPERIMENT

Using the TDPAC technique, as described below, we have measured both the magnetic hyperfine fields (MHFs) and the EFG introducing well-known nuclear probes ^{111}In/^{111}Cd at Zr and Zn sites of the $ZrZn_{1.9}$ polycrystalline sample synthesized at high pressure. Earlier we have demonstrated that our measured spectra of angle anisotropy are more well defined for this stoichiometry [25] (we observed 100% absorption of the introduced ^{111}In/^{111}Cd impurities in the crystal lattice of $ZrZn_{1.9}$). The synthesized samples for that composition (i.e., $ZrZn_{1.9}$) are characterized by the highest and most reproducible transition temperature [26] (i.e., T_c is reproducible up to 0.5 K) among all considered nonstoichiometry compounds.

The parent isotope ^{111}In with high specific activity was obtained using the ^{109}Ag(α,2n) ^{111}In reaction by irradiating a silver foil in the 32-MeV α beam at the Nuclear Physics Institute cyclotron (Moscow State University). The ^{111}In has a long enough half-life $T_{1/2} = 2.83$ d which permits carrying out experiments during up to two weeks using one portion of the initial activity. After the electron capture decay of ^{111}In, ^{111}Cd is formed in the 420-keV excited state, which de-excites by the γ-ray cascade 173–247 keV. The intermediate 247-keV state has the spin $I = 5/2$, electric quadrupole moment $Q = 0.83$ b, and $T_{1/2} = 85$ ns. Small pieces of the irradiated foil of Ag ($m < 1$ mg) have been melted together with powdered Zr and Zn (with chemical purity of 99.99% and 99,999%, respectively, and a total mass 500 mg) in ratio 1:1.9 at a pressure of 8 GPa. The ingots were crushed and small bright fragments from the inner parts of the ingots were used for the TDPAC experiments. After the ^{111}In activity had practically decayed out, the x-ray diffraction of the samples was measured. All samples had a pure cubic $C15$ Laves phase structure.

$ZrZn_2$ is crystallized in the cubic $C15$ lattice structure with Zr and Zn forming two sublattices; Fig. 1. All sites within each of the sublattices are equivalent. The local symmetry of the zirconium site is tetrahedral (the $23 \equiv T_h$ site symmetry), and that of the zinc site is rhombohedral (the $3m$ site symmetry). This difference in symmetry is instrumental in assigning the probes among two sublattices. While the tensor of the electric-field gradient (EFG) is nonzero at the Zn sites, it vanishes at all Zr sites. Consequently, at $T > T_c$ a finite electric quadrupole interaction (QI) is expected for ^{111}Cd at the Zn site and zero at the Zr site. Thus, at $T < T_c$ the ^{111}Cd probe at the Zn site experiences both the electric field gradient (EFG) and the magnetic hyperfine field (MHF), which couple to the nuclear

electric quadrupole ($Q = 0.83$ b) and the magnetic dipole (μ) moment of the intermediate nuclear state, respectively. In the proper reference frame (with the diagonal components of the tensor V_{ij} of EFG) the Hamiltonian for such static interactions reads

$$H = \frac{\hbar\omega_0}{6}\left(3I_z^2 - I(I+1) + \frac{1}{2}\eta(I_+^2 + I_-^2)\right) + \vec{\mu}\vec{B}_{\rm hf}. \quad (1)$$

Here $\omega_0 = 3eQV_{zz}/[2I(2I-1)\hbar]$ is the fundamental precession frequency, I represents the nuclear spin of the probe intermediate state ($I = 5/2$ for ^{111}Cd), the asymmetry parameter $\eta = (V_{xx} - V_{yy})/V_{zz}$, $V_{ii} = \partial^2 V/\partial^2 i$ $(i = x,y,z)$ are the principal-axis components ($|V_{zz}| \geqslant |V_{yy}| \geqslant |V_{xx}|$) of the EFG tensor, $\vec{B}_{\rm hf}$ is the magnetic hyperfine field. Finally, $\omega_L = 2\pi\nu_L = -g\mu_N B_{\rm hf}/\hbar$ is the Larmor frequency and the g factor of the $I = 5/2$ state of ^{111}Cd is [27] $g = -0.306$.

The time evolution of the perturbed $\gamma - \gamma$ correlation is described by the experimental function $R(t)$, where t is the time spent by the nucleus in the ^{111}Cd intermediate state. For a hyperfine interaction, $R(t)$ may be expanded as [28]

$$R(t) = \sum A_{kk} G_{kk}(t), \quad (2)$$

where A_{kk} are the angular correlation coefficients. The perturbation factor $G_{kk}(t)$ is a signature of the fields interacting with the probes. Here, we restrict ourselves by the perturbation parameter of the second order since the unperturbed angular correlation coefficient $A_{44} \ll A_{22}$ ($A_{22} = -0.18$). The perturbation factor $G_{22}(t) = \sum_i p_i G_{22}^i(t)$, where p_i are partial populations of different sites, $\sum_i p_i = 1$, describes a nuclear spin precession due to a hyperfine interaction. It was determined in a usual way from the angular anisotropy $R(t)$:

$$R(t) = -A_{22}Q_2G_{22}(t). \quad (3)$$

$R(t)$ was obtained by combining the delayed coincidence spectra $N(90^\circ,t)$ and $N(180^\circ,t)$ measured at the angles of 90° and 180° between detectors, respectively:

$$R(t) = -2[N(180^\circ,t) - N(90^\circ,t)]/[N(180^\circ,t) + 2N(90^\circ,t)]. \quad (4)$$

Here $Q_2 \approx 0.80$ is the solid-angle correction.

The TDPAC measurements were carried out using a four-detector spectrometer [29] equipped with an optical four-window cryostat JANIS (model SHI-950). The modified channel of cryostat had the high-pressure chamber of piston-cylinder type [30], capable of generating a sample pressure of 2 GPa. The hyperfine interaction parameters were extracted from the measured perturbation functions $A_{22}G_{22}(t)$ using the DEPACK program developed by Lindgren [31]. Magnetic ac susceptibility was measured in a piston-cylinder type pressure chamber [30] in the sample which was used for TDPAC measurements.

III. RESULTS AND DISCUSSION

The interactions of the magnetic hyperfine fields with the magnetic dipole moment of the $I = 5/2$, 245-keV state of ^{111}Cd probes situated at zirconium and zinc sites of $ZrZn_{1.9}$ were determined from the time dependence of the anisotropy $R(t)$ of ^{111}Cd at different temperatures. Figure 2 illustrates the typical thermal evolution of the TDPAC spectra (notice that the transition temperature is $T_C = 23$ K). The Fourier transform of $R(t)$ at the temperature 4 K and normal pressure is shown in Fig. 3.

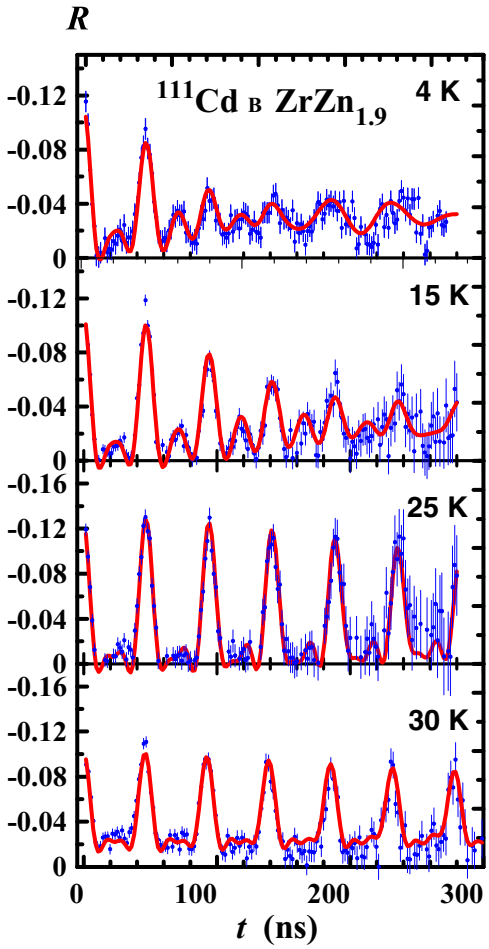

FIG. 2. (Color online) Time spectra of the angular correlation anisotropy, $R(t)$ for ^{111}Cd in $ZrZn_{1.9}$ measured at various temperatures and normal pressure ($T_C = 23$ K).

The ^{111}Cd-TDPAC spectrum measured at normal pressure and the temperature of 4 K indicates that about 30% of the ^{111}Cd nuclear probes are located at the Zr sites, while the remaining nuclear probes (about 70%) occupy the Zn sites. The probe at the Zr site having the tetrahedral symmetry (cubic site, i.e., no EFG) is described by a single Larmor frequency $\nu_{L,\rm Zr}$ (zirconium site) = 21.3(3) MHz, which corresponds to the magnetic hyperfine field $B_{Zr} = 9.2(1)$ T ($B_{HF} = 2\pi\nu_L\hbar/g\mu_N$). The ^{111}Cd probe at the zinc site in addition experiences the nuclear quadrupolar interaction with EFG and the induced magnetic hyperfine field (IMHF), related with conduction electron polarization caused by moments of neighboring ions of zirconium. At the zinc site the quadrupole frequency $\nu_{Q,\rm Zn}$ is 141(1) MHz with $\eta = 0$ [which corresponds to the EFG $V_{zz} = \nu_Q h/eQ = 7.0(2) \times 10^{17}$ V/sm^2], and the induced Larmor frequency $\nu_{L,\rm Zn}$ = 2.5(3) MHz [$B_{\rm Zn} = 1.20(14)$ T]. The quadrupole frequency $\nu_{Q,\rm Zn}$ was practically the same in the whole temperature range at normal and high pressure.

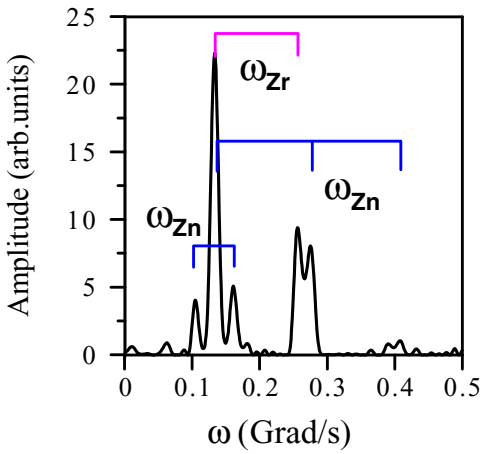

FIG. 3. (Color online) Fourier transforms of the angular correlation anisotropy time spectra $R(t)$ for ^{111}Cd in $ZrZn_{1.9}$ measured at the temperature 4 K and normal pressure. Peaks marked as ω_{Zn} and ω_{Zr} correspond to fractions with the Larmor frequencies of probes in the zinc and zirconium sublattices, respectively. The Larmor frequency for the zinc sublattice is shifted to the region of high frequencies as a result of combined interactions with a large electric field gradient (EFG), i.e., with a large quadrupolar frequency. Peaks marked as ω_{Zn} correspond to fractions with three frequencies for probes at zinc sites.

In [16] it has been demonstrated that the $4d$ and $5p$ contributions to magnetization at the Zr site amounts to 57% while the remaining part of does not lead to Bragg scattering at finite angles. The authors explain that by a contribution to magnetization which is not connected with the Zr band electrons. This however does not exclude hybridization between $4d$ states of Zr and polarized $4p$ states of Zn. The hybridization leads to induced magnetization at the Zn site and results in induced magnetic hyperfine field (IMHF) B_{Zn}. Notice also that in Refs. [15,16] spin density was detected not only at Zr sites but also at midway positions of the Zr atoms at $z = 0(1/2)$ and at $z = (3/4)$. This indicates that four tetrahedra formed by Zn atoms around a Zr site experience a homogeneously distributed magnetization from hybridized Zr $4d(T_{2g})$: Zr $5p$ electron states [16], which also leads to IMHF B_{Zn} at the Zn site.

From the fitting analysis we also extract information concerning angles β and γ giving the direction of the magnetic hyperfine field in the interaction coordinate system defined by the EFG tensor (see inset in Fig. 1). Since for the $C15$ Laves phase the principal axis of V_{zz} coincides with the crystallographic [111] axis [25], these angles define the direction of the IMHF with respect to the [111] axis. We have obtained $\beta = 51(5)^\circ$ while γ can have any value. This indicates that most likely vectors of IMHF form a cone defined by the angle β, which approximately coincides with the angle between the crystallographic [100] and [111] axes, i.e., $(54^\circ 44')$; see Fig. 1. The proposed ferromagnetic interaction [9,10,24] allows us to assume that the magnetic hyperfine field B_{Zr} at neighboring zirconium sites is parallel to IMHF at zinc sites. Later we will use this observation for deducing the magnetic structure of $ZrZn_2$.

Earlier, in $ZrZn_2$ the magnetic hyperfine field (MHF) of -1.7 T was reported at 4.2 K [21] measured with the TDPAC spectroscopy at probe ^{181}Ta nuclei placed at zirconium sites. However, probe nuclei with an open electron shell (like Ta) are not a good choice, because they substantially modify the local d-s polarization of zirconium valence electrons and inevitably distort the resultant magnetic hyperfine field.

Note also that the values of MHF determined by NMR and TDPAC spectroscopy at the ^{91}Zr nucleus and the ^{111}Cd probe nucleus, correspondingly, are different. Indeed, in the paramagnetic temperature range of $ZrZn_2$ NMR can determine only the coupling constant $A(4d) = H_{hf}(d)/\mu_B$, describing the $4d$ contribution. [Here $A(4d)$ is found from Knight shifts $K_d(T) = H_{hf}(d)\chi_d(T)/\mu_B$, and the magnetic susceptibility of d-electrons $\chi_d(T) = \chi(T) - \chi_{dia} - \chi_{orb} - 2/3\chi_s - 2\chi^{Zn}$ for $^{91}ZrZn_2$, Ref. [20]]. In order to find $A(4d)$ in the ferromagnetic temperature range one has to know the dependence of $A(4d)$ on external magnetic field and its value at zero magnetic field (see details in Ref. [20]). The extracted value of $A(4d)$ is approximately an order of magnitude smaller than the $4d$ constants for Rh and Pd [20]. The authors attributed the low value of $A(4d)$ to the negative contribution to MHF from the polarization of s electrons as a result of the s-d hybridization and the s-d exchange. These contributions are different in the case of ^{111}Cd probe in the TDPAC measurements, because the electron core of ^{111}Cd is not polarized. Therefore, the values of MHF measured at ^{91}Zr nuclei in the NMR method differ from the values of MHF measured at ^{111}Cd probe nuclei in the TDPAC spectroscopy. In general, TDPAC has the advantage over zero-field NMR that it does not require a frequency sweep to explore the distribution of MHF and has greater sensitivity and resolution than the Mössbauer effect, or γ-ray asymmetries (method of nuclear orientation).

The temperature dependence of the MHF for ^{111}Cd at the Zr site and at the Zn site is shown in Fig. 4. While the magnetic hyperfine field B_{Zr} at zirconium sites remains constant up to the Curie temperature T_C, induced MHF B_{Zn} at zinc sites demonstrates a remarkable decrease disappearing at T_C. The drop of IMHF B_{Zn} is caused by a decrease of the number of magnetically ordered zirconium ions or alternatively by a growth of the volume of the paramagnetic

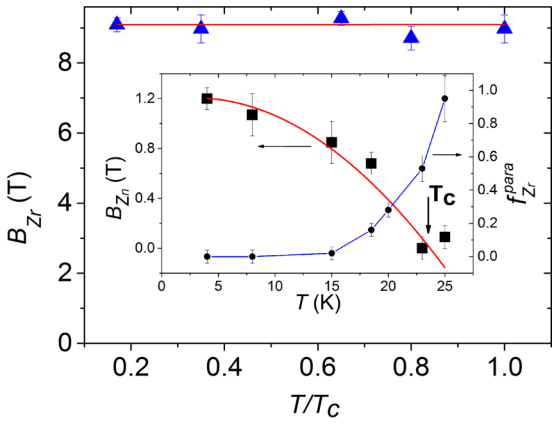

FIG. 4. (Color online) Temperature dependence of the magnetic hyperfine field B_{Zr} (▲) ($B_{hf} = 2\pi\nu_L\hbar/g\mu_N$) at probe ^{111}Cd nuclei at zirconium sites. Inset: temperature dependence of IMHF B_{Zn} (■) at probe ^{111}Cd nuclei at zinc sites and variation of the paramagnetic (fluctuating) fraction $f_{Zr}^{para}(T)$ of the zirconium sublattice (see text for details).

phase (or fast fluctuating phase) of the zirconium sublattice. This is accompanied by a fall of electron magnetic polarization at all zinc sites. The relative change of the paramagnetic phase with temperature defined as $f_{\mathrm{Zr}}^{\mathrm{para}}(T) = 1 - f_{\mathrm{Zr}}^{\mathrm{mag}}(T)$ [where $f_{\mathrm{Zr}}^{\mathrm{mag}}(T) = p_{\mathrm{Zr}}(T)/p_{\mathrm{Zr}}(0)$] is shown in the inset of Fig. 4. Notice that the thermal variation of the magnetic hyperfine field, which drops abruptly from 9 T at 22 K to 0 at 23 K, strongly suggests that the transition has a pronounced first-order character. The coexistence of ordered and fluctuating/paramagnetic states is also a typical feature of a first-order transition.

In this paragraph we briefly discuss the character of the phase transition. Despite theoretical conclusions that the phase transition in weak itinerant ferromagnets, i.e., in systems with a very low T_{C}, can be fluctuation-induced first order [32–35], reliable experimental confirmations of weak first-order transitions begin to appear only in the last 20 years. In high-pressure experiments for MnSi it has been shown that the helimagnetic transition there is second order for pressures $p < p^* \sim 1.2$ GPa and is weakly first order in the range $p^* < p < p_c \approx 1.46$ GPa [36]. Later, by means of specific heat, thermal expansion, electrical resistivity [37], and ultrasound experiments [38], Stishov *et al.* have demonstrated that the transition in MnSi at normal pressure is indeed of first order with a tiny latent heat. Recently, on the basis of neutron-scattering data and the thermodynamical Dzyaloshinskii-Moriya model, Janoschek *et al.* [39] have confirmed that such a fluctuation-induced first-order transition is realized in MnSi between its paramagnetic and helimagnet state. As a result, it can be considered as proven that in MnSi, which is in many aspects analogous to $ZrZn_2$, the magnetic transition is not of second order, but fluctuation-induced first order. MnSi is not unique in that respect. In the novel helimagnetic compound MnGe by means of Mössbauer effect has also been shown the occurrence of the fluctuation-induced first-order magnetic transition [40]. Nowadays, it is known that at high pressure $ZrZn_2$, which is also a system with strong spin fluctuations [41], behaves similarly to MnSi [9]. In $ZrZn_2$ the ordered ferromagnetic moment disappears discontinuously at $p_c = 1.65$ GPa and a tricritical point separates a line of first-order ferromagnetic transitions from second-order transitions at higher temperature [9]. Therefore, one cannot rule out that the first-order transition which we observe at normal pressure in our TDPAC experiments is fluctuation-induced transition like in MnSi. Note also that in our experiments we study the nonstehiometric compounds $ZrZn_{1.9}$ with a lowered temperature of magnetic ordering, which can possibly influence the order of the transition. Earlier, the ^{111}Cd-TDPAC method was used by Forker *et al.* [42,43] to study cubic Laves phases of RCo_2, where R is a rare-earth element. It has been found that for heavy lanthanides (starting from Dy) the magnetic ordering transition from the paramagnetic phase to the ferrimagnetic one is of first order. This transition is metamagnetic for cobalt sublattice [44]. In particular, the temperature dependence of the magnetic hyperfine field and the character of the transition to the paramagnetic phase in $PrCo_2$ and $NdCo_2$ are indicative of the first-order transition although measurements performed with other methods conclude that the transition is of second order [45,46]. However, the Curie temperatures and the induced magnetic moments of Co for $PrCo_2$ and

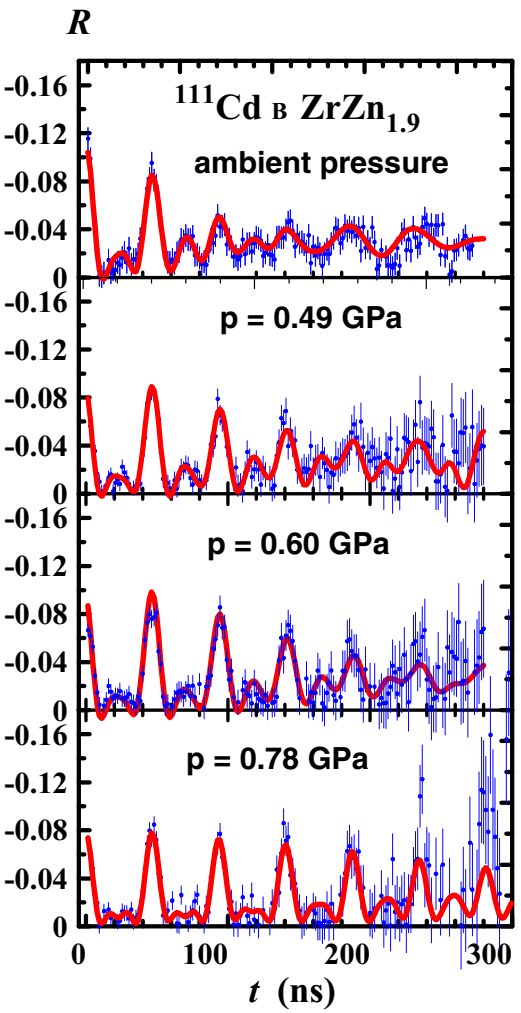

FIG. 5. (Color online) Time spectra of the angular correlation anisotropy $R(t)$ for ^{111}Cd in $ZrZn_{1.9}$ measured at various pressures and the temperature $T = 4$ K.

$NdCo_2$ are comparable with the values for RCo_2 with heavy rare-earth elements R. On the other hand, in [44] it has been shown that according to the theory [47] the substitution of terbium by yttrium in $Tb_{1-x}Y_xCo_2$ leads to the lowering of its Curie temperature and the character of the transition changes from second order to first order. Therefore, in terms of first order–second order $PrCo_2$ and $NdCo_2$ are probably boundary compounds and depending on synthesis conditions can expose either order of magnetic transition. Our finding on the character of the phase transition in $ZrZn_2$ apparently requires further investigation and confirmation.

The pressure evolution of the TDPAC spectra measured at $T = 4$ K is shown in Fig. 5. At the pressure $P = 0.78$ GPa and above we found that Larmor frequencies $\nu_{L,\mathrm{Zr}} = 0$ and $\nu_{L,\mathrm{Zn}} = 0$. Pressure dependencies of the magnetic hyperfine fields B_{Zr} and B_{Zn} when $P < 0.78$ GPa are plotted in Fig. 6. While MHF B_{Zr} at the zirconium site does not change up to 0.6 GPa, induced MHF B_{Zn} at the zinc site decreases linearly. At a pressure above 0.6 GPa both B_{Zr} and B_{Zn} drop discontinuously. This indicates that IMHF B_{Zn} (and electron magnetic polarization at all Zn sites) depends on interatomic

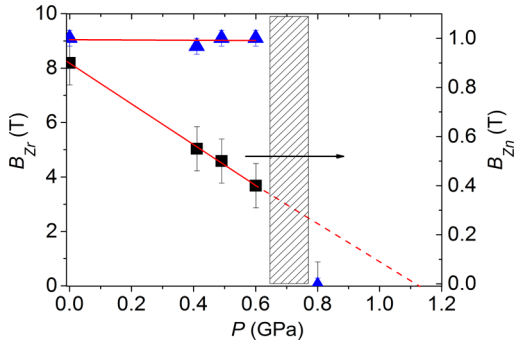

FIG. 6. (Color online) Pressure dependencies of the magnetic hyperfine fields B_{Zr} and B_{Zn} measured at the temperature $T = 4$ K for the probe ^{111}Cd nucleus at the zirconium and zinc sites in $ZrZn_{1.9}$. (▲) data for the zirconium site (B_{Zr}) and (■) data for the zinc site (B_{Zn}).

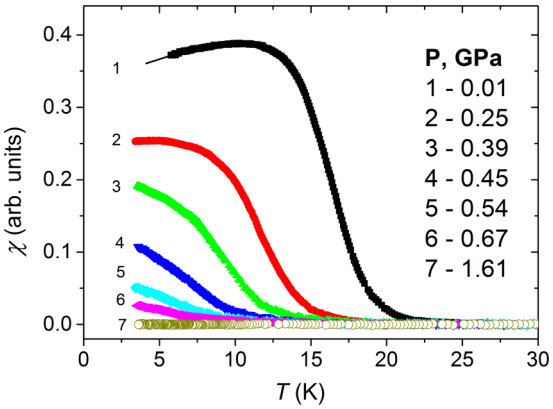

FIG. 8. (Color online) Temperature dependencies of the magnetic ac susceptibility of $ZrZn_{1.9}$ measured at pressures up to 1.61 GPa and temperatures down to 4.2 K.

distances, while B_{Zr} at zirconium sites may be responsible for the first-order quantum phase transition [9] observed in $ZrZn_2$ at a high pressure.

Figure 7 illustrates the pressure evolution of the Curie temperature T_C for the same sample of $ZrZn_{1.9}$ measured by ^{111}Cd-TDPAC technique and magnetic ac susceptibility. One can clearly see a good correspondence between these two methods. The difference in values of T_C can be explained by the fact that the microscopic (TDPAC) method has a higher sensitivity to the local changes of magnetic interactions.

Figure 8 shows the temperature dependence of the magnetic ac susceptibility of $ZrZn_{1.9}$ measured at pressures up to 1.61 GPa and temperatures down to 4.2 K. (Here we have used a miniature chamber of the piston-cylinder type [30].) As pressure increases up to 0.4 GPa the Curie temperature T_C of $ZrZn_{1.9}$ reduces linearly. For pressures above 0.4 GPa the Curie temperature T_C exhibits a nonlinear dependence with a sudden drop. It has been demonstrated previously that polycrystalline samples of $ZrZn_2$ synthesized at high pressure show basically the pressure evolution reported for $ZrZn_2$ earlier albeit they are also highly sensitive to the quality and the history of

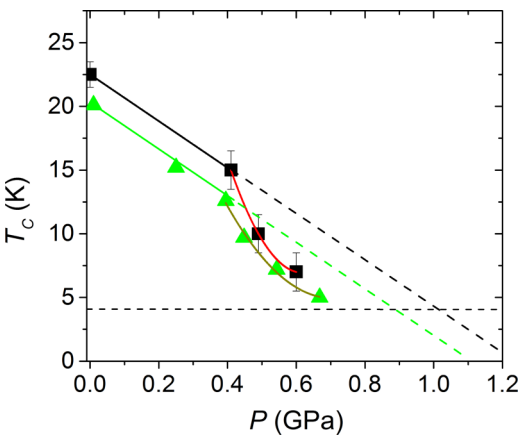

FIG. 7. (Color online) Pressure dependencies of Curie temperature T_C for the same sample of $ZrZn_{1.9}$ (■) data of the ^{111}Cd-TDPAC measurements and (▲) the magnetic ac susceptibility measurements (see also Fig. 8).

samples [48]. Therefore, the deviation from the linear decrease of T_C in $ZrZn_{1.9}$ is most likely caused by vacancies which lead to a decrease of the exchange interaction.

Ab initio calculations of the hyperfine field on Cd impurities with scaled exchange-correlation potential (as in Ref. [49]) yield the coupling constants $A_{Zr} = -18.4T/\mu_B$ for the Cd probe located at the zirconium site and $A_{Zn} - 4.2T/\mu_B$ for Cd at the zinc site [50]. Although the calculations [50] depend on the approximation used for the exchange-correlation term within DFT, they demonstrate a linear dependence between the calculated magnetic moment and magnetic field, so that coupling constants characterize the dependencies quite well. It is worth noting that earlier the magnetic hyperfine field B_{hf} was found to be approximately proportional to the inducing d moment in the $3d$ hosts Fe, Co, Ni [51,52]: for the closed-shell nucleus ^{111}Cd, e.g. B_{hf} was a linear function of μ_{3d} with the coupling constant $A_{3d} = B_{hf}/\mu_{3d} = -18T/\mu_B$ [53]. There is a good correspondence between the coupling constant obtained from the calculation of the zirconium sublattice of $ZrZn_2$ and the constant found from experiments for $3d$ hosts Fe, Co, Ni. This observation gives us a certain justification for further analysis. With experimental values of magnetic hyperfine field at zirconium sites measured at ^{111}Cd nuclei by TDPAC and the calculated coupling constant we can estimate the magnetic moment at the zirconium site in $ZrZn_{1.9}$. We have obtained $\mu_{Zr} = 0.50(3)\mu_B$. Since IMHF B_{Zn} at the zinc site is quite small and determined with the experimental accuracy of approximately 10% and in addition there are no experimental data on its coupling constant, the analysis of the induced magnetic moment at zinc sites will be omitted.

Our estimation for coupling constants and the magnetic moment of zirconium is in contradiction with the measured net macroscopic moment of $ZrZn_2$ which according to previous studies lies in the range 0.13–0.23μ_B/f.u. The question on magnetic structure of $ZrZn_2$ then arises: Obviously, it should be a complex one because the simple ferromagnetic order does not fit our data. However, search of a short-pitch spiral or ferrimagnetic solution in *ab initio* calculations [50] was unsuccessful and the only stable configuration was ferromagnetic with sizable magnetization. Earlier, direct full-potential LDA calculations of Mazin *et al.* [24] gave the value of

magnetic moment which is three to four times larger than the value obtained from magnetization measurements. The agreement with magnetization data was restored only if fluctuation-renormalized Landau theory is included in the calculation procedure. Spin fluctuations thus tend to reduce the magnetic moment. However, in local TDPAC measurements the characteristic time is only 10^{-8} s, which implies that low-frequency spin fluctuations are ineffective, which can possibly explain a larger value of the magnetic moment of zirconium deduced from our TDPAC measurements.

As we have already discussed earlier, the measured induced MHF B_{Zn} at the zinc site allows us to determine the orientation of MHF B_{Zr} in respect to the [111] crystallographic axis and consequently the direction of the magnetic moment of zirconium; see Fig. 1. Therefore, we can suggest that magnetic moments of zirconium ions form a conical magnetic structure, which is characterized by a ferromagnetic component $\mu^{\parallel}$ parallel to the [111] axis and a component $\mu^{\perp}$ perpendicular to it making a spiral.

Notice that exactly the same question was posed by zero-field muon-spin-rotation experiments, which have provided evidence for an antiferromagnetic component in the magnetic structure of $ZrZn_2$ [23]. It is also known that the zero-field magnetic structure of $CeAl_2$ which is isostructural to $ZrZn_2$, is a nonchiral spiral [54]. On the basis of these considerations we suggest that in $ZrZn_{1.9}$ ($ZrZn_2$) a conical structure of zirconium magnetic moments with a long-pitch spiral is realized. Indeed, the ferromagnetic [111] component with the angle $\beta = 54^{\circ}$ results in $0.3\mu_B$/Zr, which lies closer to the observable net magnetization [9,10], and is also supported by the fact that the [111] axis coincides with the easy direction of magnetization [55].

IV. CONCLUSIONS

We have performed accurate TDPAC measurements of hyperfine magnetic field and electric-field gradient on the ^{111}Cd substitutional nuclei at zirconium and zinc sites in $ZrZn_{1.9}$.

From the TDPAC data we have extracted values of the magnetic hyperfine field B_{Zr} at the zirconium site and induced MHF B_{Zn} at the zinc site. We have measured their temperature dependence at normal pressure and the dependence on external pressure at 4 K. We have found that the transition to the magnetically ordered structure is of first order not only at high but also at normal pressure. Based on the orientation of IMHF B_{Zn} in respect to the EFG principal axis V_{zz} we have made conclusions concerning the orientation of zirconium magnetic moment μ_{Zr}.

Using *ab initio* electron band-structure calculations [50], experimental data on the magnetic field–moment coupling constant [51,52] and experimentally measured MHF B_{Zr} at the zirconium site we have estimated the magnetic moment μ_{Zr} of zirconium. We have found $\mu_{Zr} = 0.50(3)\mu_B$, which is substantially larger than what has been believed so far. Thus, our experimental data as well as muon spin rotation experiments [23] giving evidence for an antiferromagnetic component in the magnetic structure of $ZrZn_2$ have led us to suggest that the magnetic ordering in $ZrZn_2$ has a conical structure of zirconium magnetic moments with a long-pitch spiral.

Further studies of $ZrZn_2$ with methods that can selectively determine local magnetic properties are needed to determine the details of its magnetic order.

ACKNOWLEDGMENTS

The authors are grateful to S. M. Stishov, V. B. Brudanin, N. G. Chechenin, and N. N. Delyagin for support of this work. We are also grateful to I. I. Mazin for useful discussions and an opportunity to use his unpublished data. The work was supported by the Russian Foundation for Basic Research (Grant No. 14-02-00001) and by special programs of the Department of Physical Science, Russian Academy of Sciences. The work at the Joint Institute for Nuclear Research was carried out under the auspices of a Polish representative in the JINR.

[1] G. Stewart, Rev. Mod. Phys. **73**, 797 (2001).
[2] S. S. Saxena, P. Agarwal, K. Ahilan, F. M. Grosche, R. K. W. Hasselwimmer, M. J. Steiner, E. Pugh, I. R. Walker, S. R. Julian, P. Monthoux, G. G. Lonzarich, A. Huxley, I. Sheikin, D. Braithwaite, and J. Flouquet, Nature (London) **406**, 587 (2000).
[3] A. Huxley, I. Sheikin, E. Ressouche, N. Kernavanois, D. Braithwaite, R. Calemczuk, and J. Flouquet, Phys. Rev. B **63**, 144519 (2001).
[4] D. Fay and J. Appel, Phys. Rev. B **22**, 3173 (1980).
[5] K. Miyake, S. Schmitt-Rink, and C. M. Varma, Phys. Rev. B **34**, 6554 (1986).
[6] V. Taufour, D. Aoki, G. Knebel, and J. Flouquet, Phys. Rev. Lett. **105**, 217201 (2010).
[7] M. Lee, W. Kang, Y. Onose, Y. Tokura, and N. P. Ong, Phys. Rev. Lett. **102**, 186601 (2009).
[8] R. Ritz, M. Halder, C. Franz, A. Bauer, M. Wagner, R. Bamler, A. Rosch, and C. Pfleiderer, Phys. Rev. B **87**, 134424 (2013).
[9] M. Uhlarz, C. Pfleiderer, and S. M. Hayden, Phys. Rev. Lett. **93**, 256404 (2004).
[10] M. Uhlarz, C. Pfleiderer, H. v. L. ohneysen, S. Hayden, and G. Lonzarich, Physica B **312**, 487 (2002).
[11] N. Kernavanois, B. Grenier, A. Huxley, E. Ressouche, J. P. Sanchez, and J. Flouquet, Phys. Rev. B **64**, 174509 (2001).
[12] Y. Ishikawa, K. Tajima, D. Bloch, and M. Roth, Solid State Commun. **19**, 525 (1976).
[13] M. Ishida, Y. Endoh, S. Mitsuda, Y. Ishikawa, and M. Tanaka, J. Phys. Soc. Jpn. **54**, 2975 (1985).
[14] G. Shirane, R. Cowley, C. Majkrzak, J. B. Sokoloff, B. Pagonis, C. H. Perry, and Y. Ishikawa, Phys. Rev. B **28**, 6251 (1983).
[15] S. J. Pickart, H. A. Alperin, G. Shirane, and R. Nathans, Phys. Rev. Lett. **12**, 444 (1964).
[16] P. J. Brown, K. R. A. Ziebeck, and P. G. Mattocks, J. Magn. Magn. Mater. **42**, 12 (1984).

[17] N. R. Bernhoeft, S. A. Law, G. G. Lonzarich, and D. M. Paul, Phys. Scr. **38**, 191 (1988).
[18] T. Yamadaya and M. Asanuma, Phys. Rev. Lett. **15**, 695 (1965).
[19] S. Ogawa and N. Sakamoto, J. Phys. Soc. Jpn. **22**, 1214 (1967).
[20] M. Kontani, T. Hioki, and Y. Masuda, J. Phys. Soc. Jpn. **39**, 665 (1975)
[21] I. S. Barrett and J. A. Cameron, J. Phys. C: Solid State Phys. **9**, 1303 (1976).
[22] B. T. Murdoch, C. E. Olsen, and W. A. Steyert, Phys. Lett. A **44**, 413 (1973).
[23] P. Dalmas der Réotier, G. Lapertot, A. Yaouanc, P. C. M. Gubbens, S. Sakarya, and A. Amato, Phys. Lett. A **349**, 513 (2006).
[24] I. I. Mazin and D. J. Singh, Phys. Rev. B **69**, 020402(R) (2004).
[25] A. A. Sorokin, G. K. Ryasny, B. A. Komissarova, L. N. Fomicheva, A. V. Tsvyashchenko, and S. M. Nikitin, Hyperfine Interact. **171**, 269 (2006).
[26] G. S. Knapp, F. Y. Fradin, and H. V. Culbert, J. Appl. Phys. **42**, 1341 (1971).
[27] G. Schatz and A. Weidinger, *Nucl. Condens. Matter Phys.* (Wiley & Sons, Ltd., Sussex, 1996).
[28] R. M. Steffen and H. Frauenfelder, in *Perturbed Angular Correlations*, edited by E. Karlsson, E. Matthias, and K. Siegbahn (North-Holland, Amsterdam, 1963).
[29] V. B. Brudanin, D. V. Flossofov, O. I. Kochetov, N. A. Korolev, M. Milanov, V. Ostrovskiy, V. N. Pavlov, A. V. Salamatin, V. V. Timkin, A. I. Velichkov, L. N. Fomicheva, A. V. Tsvyashchenko, and Z. Z. Akselrod, Nucl. Instrum. Methods Phys. Res. A **547**, 389 (2005).
[30] A. N. Voronovski, E. M. Dizhur, and E. S. Itskevich, Zh. Eksp. Teor. Fiz. **77**, 1119 (1979) [Sov. Phys. JETP **50**, 564 (1979)].
[31] B. Lindgren, Hyperfine Interact. C **1**, 613 (1996).
[32] S. A. Brazovskii, I. E. Dzyaloshinski, and B. G. Kukharenko, Zh. Eksp. Teor. Fiz. **70**, 2257 (1976) [Sov. Phys. JETP **43**, 1178 (1976)].
[33] I. E. Dzyaloshinski, Zh. Eksp. Teor. Fiz. **72**, 1930 (1977) [Sov. Phys. JETP **45**, 1014 (1977)].
[34] P. Bak and M. H. Jensen, J. Phys. C **13**, L881 (1980).
[35] D. Belitz, T. R. Kirkpatrick, and T. Vojta, Phys. Rev. Lett. **82**, 4707 (1999).
[36] C. Pfleiderer, G. J. McMullan, S. R. Julian, and G. G. Lonzarich, Phys. Rev. B **55**, 8330 (1997).
[37] S. M. Stishov, A. E. Petrova, S. Khasanov, G. Kh. Panova, A. A. Shikov, J. C. Lashley, D. Wu, and T. A. Lograsso, Phys. Rev. B **76**, 052405 (2007).
[38] A. E. Petrova and S. M. Stishov, J. Phys.: Condens. Matter **21**, 196001 (2009).
[39] M. Janoschek, M. Garst, A. Bauer, P. Krautscheid, R. Georgii, P. Böni, and C. Pfleiderer, Phys. Rev. B **87**, 134407 (2013).
[40] M. Deutsch, P. Bonville, A. V. Tsvyashchenko, L. N. Fomicheva, F. Porcher, F. Damay, S. Petit, and I. Mirebeau, Phys. Rev. B **90**, 144401 (2014).
[41] S. J. C. Yates, G. Santi, S. M. Hayden, P. J. Meeson, and S. B. Dugdale, Phys. Rev. Lett. **90**, 057003 (2003).
[42] M. Forker, S. Müller, P. de la Presa, and A. F. Pasquevich, Phys. Rev. B **68**, 014409 (2003).
[43] M. Forker, S. Müller, P. de la Presa, and A. F. Pasquevich, Phys. Rev. B **75**, 187401 (2007).
[44] R. Z. Levitin and A. S. Markosyan, Usp. Fiz. Nauk **155**, 623 (1988).
[45] J. Herrero-Albillos, F. Bartolome, L. M. Garcia, F. Casanova, A. Labarta, and X. Batlle, Phys. Rev. B **73**, 134410 (2006).
[46] J. Herrero-Albillos, F. Bartolome, L. M. Garcia, F. Casanova, A. Labarta, and X. Batlle, Phys. Rev. B **75**, 134410 (2007).
[47] D. Bloch, M. Edwards, M. Shimizu, and J. Voiron, J. Phys. F: Met. Phys. **5**, 1217 (1975).
[48] S. M. Stishov, V. A. Sidorov, A. V. Tsvyashchenko, E. D. Bauer, A. E. Petrova, T. Park, and J. D. Thompson, Physica B **378**, 411 (2006).
[49] A. Aguayo, I. I. Mazin, and D. J. Singh, Phys. Rev. Lett. **92**, 147201 (2004).
[50] I. I. Mazin (private communication). Actual calculations were performed by the linear augmented plane method, as implemented in the WIEN2K code, in the local-density approximation with or without gradient corrections. In both cases, the calculated magnetic moment on Cd was tuned by using exchange field scaling as described in Ref. [49]. Supercells with eight formula units were utilized to simulate a single Cd impurity.
[51] G. N. Rao, Hyperfine Interact. **7**, 141 (1979).
[52] K. S. Krane, Hyperfine Interact. **16**, 1069 (1983).
[53] P. de la Presa, S. Müller, A. F. Pasquevich, and M. Forker, J. Phys.: Condens. Matter **12**, 3423 (2000).
[54] E. M. Forgan, B. D. Rainford, S. L. Lee, J. S. Abell, and Y. Si, J. Phys.: Condens. Matter **2**, 10211 (1990).
[55] E. A. Yelland, S. J. C. Yates, O. Taylor, A. Griffiths, S. M. Hayden, and A. Carrington, Phys. Rev. B **72**, 184436 (2005).